IEEE Access
Multidisciplinary : Rapid Review : Open Access Journal

Received July 5, 2019, accepted July 19, 2019, date of publication July 23, 2019, date of current version August 9, 2019.

Digital Object Identifier 10.1109/ACCESS.2019.2930585

A Time-Delay Calibration Method for Profile Estimation of Two-Layered Rough Surfaces

YING LIU[1,2], (Student Member, IEEE), AND LIXIN GUO[1], (Senior Member, IEEE)
[1]School of Physics and Optoelectronic Engineering, Xidian University, Xi'an 710071, China
[2]Institute of Antenna and Microwave Techniques, Tianjin University of Technology and Education, Tianjin 300222, China

Corresponding author: Ying Liu (liuying_tute@163.com)

This work was supported in part by the National Natural Science Foundation of China under Grant 61871457 and Grant 61431010, in part by the Foundation for Innovative Research Groups of the National Natural Science Foundation of China under Grant 61621005, in part by the 111 Project under Grant B17035, in part by the Natural Science Foundation of Tianjin Municipality, China, under Grant 18JCYBJC16400, and in part by the Science Research and Development Foundation of Tianjin University of Technology and Education under Grant KJ1818.

ABSTRACT For detection of a two-layered rough surface structure through ground-penetrating radar, the estimation of the profile of each layered rough surface is an important problem to be solved. In modeling and calculating the scattering of two-layered rough surfaces, we found that the profile of the upper rough surface can be observed directly through the figure of the echo from the upper surface. However, the echo of the lower rough surface has a quite different shape from its surface profile, because of the influence of the scattering of the upper rough surface. This is disadvantageous to the estimation and imaging of the profile of the lower rough surface. To solve this problem, a time-delay calibration method is proposed in this paper to be applied to the profile estimation of the lower rough surface in the case of two-layered rough interface detection. By introducing a smooth surface, the expression of time delay is derived to eliminate the influence of the scattering of the upper surface. Applying the derived expression of time delay to the echo data from the lower rough surface, the echo outline of the lower rough surface can be corrected to reflect the surface's profile shape. The calibrated B-scan echo shape shows good agreement with the profile of the lower rough surface. With this method, we can get the profile shape of the lower rough surface quickly and simply by calibrating the echo data directly. This method can be used for fast microwave imaging of two-layered rough surface and for eliminating the interference of scattering from rough surface on the echoes of nearby targets. The purpose of this paper is to solve the problem we have found in our previous work. The work of this paper is an extension of the previous work.

INDEX TERMS Profile estimation, time-delay calibration, two-layered rough surface scattering, ground-penetrating radar, echo shape.

I. INTRODUCTION

Microwave detection of a layered structure with rough interfaces attracts many scholars' attention because of its wide applications [1]–[5], such as probing of underground rock and soil structure by ground penetrating radar (GPR) [1], [4], civil engineering [2], sea surface (snow covered sea ice) [3], [5], medical microwave imaging, road subgrade detection, and so on. Many numerical methods and approximate methods are used to compute and simulate the scattering of the stratified structure with rough interfaces for microwave detection [4]–[9].

The associate editor coordinating the review of this manuscript and approving it for publication was Davide Comite.

One of the important purposes of investigating the forward problem, i.e., the scattering of stratified rough surfaces, is to analyze the results of the detection effectively so that the profiles of the layered rough interfaces can be reconstructed. In some cases, there may also be one or more targets with unknown shapes and attributes near the rough interface. It is difficult to accurately identify and image the target because of the overlay interference of the reflected echo from the rough interface. Therefore, the estimation of the rough surface contour can often clear the obstacle for the recognition and imaging of the target near the rough surface. The profiling of the rough interface can remove clutter interference for the target, and make the target recognition and imaging more accurate.

In recent years, some scholars have studied the method of estimating and reconstructing the profile of a rough surface in the microwave detection. Akduman et al. presented an iterative method based on a Fourier transform and a Taylor expansion for reconstructing the profiles of dielectric rough surface at fixed frequency [10]. The Newton method and the regularization in the least-square sense were investigated and applied to reconstruct perfectly conducting rough surface profiles [11]. Feng et al. used a migration technique to estimate the surface profile accurately in the case of sharp variable rough surface [12]. The contrast-source-inversion method and the buried object approach were investigated to reconstruct dielectric objects buried under a rough surface [13]. The time-reversal imaging method was studied for imaging buried targets under a rough surface [14], [15]. Comite et al. presented an image-domain adaptive likelihood ratio tests detector for target detection with clutter arising from a rough interface [16].

However, these studies only focus on the estimation and reconstruction of one-layered rough surface or the top rough interface of the layered structure (the top surface is flat). For the single-layer rough surface structure, it is often simple and easy to operate to estimate the rough surface profile directly from the echoes. The wave peak pattern of echo from the rough surface can show the shape of the rough surface's profile. For example, a method of finding the brightest pixels in the GPR profile is often used to obtain accurate surface topography [12]. However, the structure of the stratified rough surface often involves two or more rough surfaces. Due to the influence of the scattering of the upper surface, the profile of the lower surface in the two-layered structure is difficult to estimate. Therefore, it is especially important to study the profile estimation of the lower surface in the two-layered rough surface structure.

In our previous work of analysis on GPR echo from the underground layered rough interfaces [17], we found that the echo from the top rough surface shows the same shape with its surface profile, but the lower rough surfaces cannot reflect the surface profiles. To solve this problem, we present a time-delay calibration method in this paper to estimate the profile of the lower rough surface in the two-layered rough surface structure. This method can eliminate the influence of the scattering of the upper surface on the echo shape of the lower surface by directly adjusting the time delay. Additionally, the calibrated wave outline of the lower-surface echo can reflect the surface profile. It is convenient to observe the lower-rough-surface profile directly from the radar echo shape and obtain the contour fluctuation information. This method is suitable for fast microwave imaging, including the concrete evaluation and the roadbed detection. Moreover, it can be further applied to target recognition and imaging near the lower rough surface, for example, mine detection.

The rest of this paper is organized as follows. Section II presents the modeling and computing methods of the scattering of layered rough interfaces. In Section III, a detailed description of the proposed time-delay calibration method is given, and the numerical results of the calibrated B-scan echoes from the lower rough interfaces are provided to prove the validity of the method. Conclusions are given in Section IV.

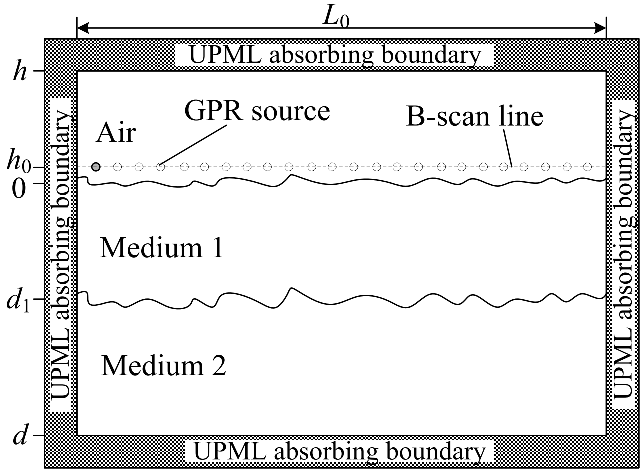

FIGURE 1. **2-D computational model for GPR detection of two-layered rough surfaces.**

II. SCATTERING MODELING

A. COMPUTATIONAL MODEL CONSTRUCTION

Fig. 1 shows the scattering model for GPR detection of an underground two-layered rough surface structure. In the model, there are three layers of medium: the layer of air, the layer of medium 1, and the layer of medium 2. The interfaces between the three layers are all rough surfaces, described as the upper rough surface (ground surface) and the lower rough surface. The GPR antenna moves along the B-scan line, sends electromagnetic waves to the ground at every sampling point, and receives echoes from underground, forming the B-scan echo data. The height of the upper rough surface is set to be 0 m, and the antenna height from the ground surface is h_0. d_1 is the depth of the layer of medium 1, and d is the total depth of the two layers of medium 1 and medium 2; thus, the depth of the layer of medium 2 is $(d - d_1)$. L_0 is the length of the B-scan line, and h is the total height of the air layer in the model. Therefore, the total dimensions of the computational model are $L_0 \times (h + d)$. And the uniaxial perfectly matched layer (UPML) is used as the outer boundary of the computing region of the model.

B. NUMERICAL METHOD

In recent years, a variety of numerical methods and approximate methods have been developed for the computation of electromagnetic scattering from layered structures and rough interfaces, such as the method of moments [18], [19], the Kirchhoff approximation method [20], the propagation-inside-layer expansion method [21], [22], the finite-difference time-domain method (FDTD) [23], [24], the small perturbation method [25], [26], and the translation matrix method [27]. For GPR, the wideband electromagnetic pulse is mostly used, and the echo data are time-domain data that are easy to observe intuitively. This is consistent with the advantages and applicability of the FDTD method. Therefore, FDTD has been recognized as one of the most effective methods for GPR simulation. In this paper, the FDTD method is used to compute the scattering of a layered rough surface in the ground penetrating model.

As a result of limited computer capacity, FDTD computation can only be made in a finite region. In order to simulate the propagation of electromagnetic waves in infinite space in a finite computational region, it is necessary to build a virtual absorbing boundary on the truncated boundary of the computational region. The absorbing boundary can make the outgoing waves propagate outward without reflection from it. In our present work, the UPML absorbing medium is used to terminate the FDTD computational region.

C. ROUGH SURFACE GENERATION

To study the electromagnetic scattering characteristics of layered rough interfaces, it is necessary to model random rough surfaces. The common method used to simulate a rough surface is the Monte Carlo method for simulating the Gaussian random rough surface [28]. The basic idea of the Monte Carlo method, also called linear filtering, is to filter the power spectrum in the frequency domain and then use inverse fast Fourier transform to get the height fluctuation of a rough surface. The Gaussian rough surface is the most typical rough surface. In simulating Gaussian rough surface, the root mean square (rms) height and correlation length are the most basic and important two parameters. Their changes have a great influence on the fluctuating height and fluctuating frequency of the rough surface respectively.

Fig. 2 shows a numerical simulation result of one-dimensional Gaussian rough surfaces with different rms heights and correlation lengths. In Fig. 2, λ represents the wavelength and Lrepresents the total length of the rough surface. As shown in Fig. 2(a), when the rms height δ remains the same ($\delta = 0.3\lambda$), a small correlation length l equates to a short changing period for the rough surface, i.e., rapid changes in the rough surface. And we can see from Fig. 2(b), when the correlation length l is invariant ($l = \lambda$), a large rms height δ equates to a large fluctuating height of the rough surface. In addition, when the rough surface is realized by Fourier inverse transformation, the total length L of the surface should have at least five correlation lengths so that the overlapping of the spectrum can be reduced.

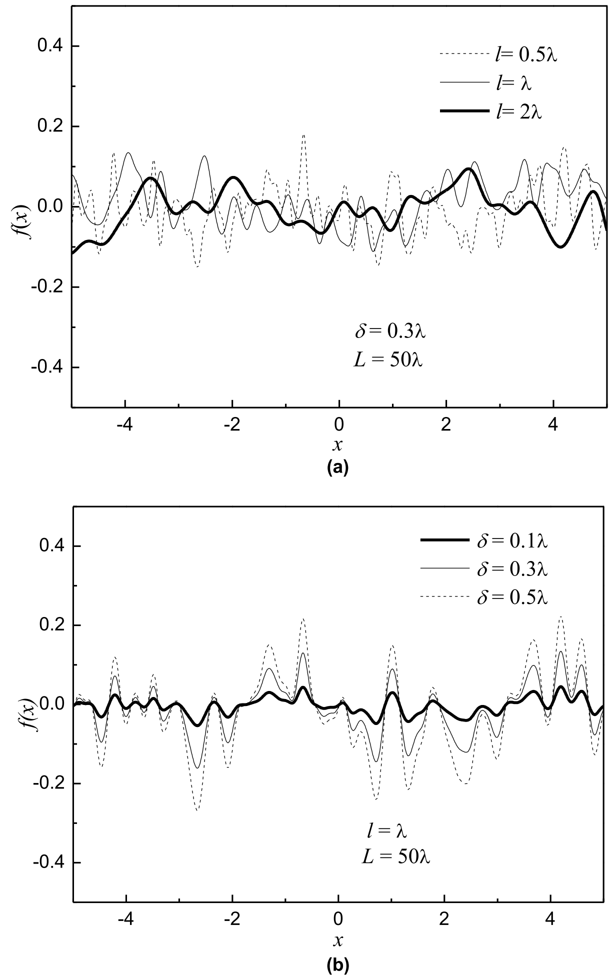

FIGURE 2. Model of a one-dimensional Gaussian randomly rough surface.

III. TIME-DELAY CALIBRATION METHOD

A. PROBLEM DESCRIPTION

In our previous work [17], we simulated the GPR B-scan echoes of two-layered rough surfaces and compared them with the profiles of the corresponding layered rough surface. From the simulation results, we found that regardless of the changes in roughness, the echo shape of the upper surface is always the same with the profile of the upper rough surface. However, when the profile of the upper rough surface is different from that of the lower rough surface, the echo shape of the lower surface is quite different from the shape of its surface profile, because of the influence of the scattering of the upper surface. In other words, the echo from the upper surface can reflect the surface's profile, whereas, the lower surface echo cannot reflect the surface's profile.

It is very convenient and fast to get the contour fluctuation of rough surface by observing the echo shape directly. So it is expected that the profile of the lower rough surface in the two-layered rough surface structure can be obtained directly by the echo shape of the lower surface. This is of practical significance and application value in engineering practice. Therefore, we need to find a way to calibrate the B-scan echo of the lower rough surface so that it can directly reflect the rough surface's profile.

B. METHODOLOGY

As we know, the B-scan echo data vary with time. The echo peak time t is closely related to the propagation velocity v of electromagnetic wave in the medium and the distance s reaches the interface, and can be written as

$$t = 2s/v \tag{1}$$

The propagation velocity v of electromagnetic wave in the medium can be calculated by

$$v = \frac{c}{\sqrt{\mu \varepsilon}} \tag{2}$$

where c is the propagation velocity of electromagnetic wave in vacuum, μ is the magnetic conductivity coefficient of the medium, and ε is the dielectric permittivity of the medium.

The time t the wave peak appears can be detected in the echo data. So if the parameters μ and ε of the medium are known, the distance of wave propagation from the sampling point to the rough interface can be calculated. Thus, the depth and the undulating profile of the rough surface can be obtained. Therefore, the B-scan echo data themselves carry the information of rough surface contours, which is very helpful for estimating the rough surface profile. However, in the echo data of two-layered rough surfaces, the echo shape of the rough surface that is below the top surface cannot reflect the rough surface's profile. This is mainly due to the roughness of the upper surface, which makes the wave travel start at different times in the lower layer. Thus, the profiles of the lower rough surface cannot be quickly estimated through the GPR echoes. Therefore, a calibration method is needed to calibrate the echo data of the lower rough surface to reflect the surface profile.

Fig. 3 shows a schematic diagram of parameters used in the time-delay calibration method for layered rough surface estimation. The GPR antenna emits electromagnetic waves vertically along the B-scan line at various sampling points and receives reflected waves from the ground. Thus, the B-scan echo data are composed of the echo signals received at each sampling point. In Fig. 3, $s_1, s_2, \ldots, s_n$ are the sample points on the B-scan line, and l_0 denotes the vertical distance between the B-scan line and the highest point of the upper rough surface. $t_a(i)$ $(i = 1, \ldots, n)$ is the time that the echo peak of the upper rough surface reaches the B-scan line at each sample point, $t_b(i)$ $(i = 1, \ldots, n)$ is the time that the echo of the lower rough surface reaches the B-scan line at each sample point. $t_{\min}$ is the minimum value of the time $t_a(i)$. $g(i)$ $(i = 1, \ldots, n)$ represents the vertical distance between each sample point on the upper rough surface and the horizontal line where the highest point of the rough surface undulates. Finally, $d(i)$ $(i = 1, \ldots, n)$ denotes the vertical distance between the upper rough surface and the lower rough surface at each sampling point.

From Fig. 3, we can see that the echoes from the upper rough surface received at the sampling points start from the point on the B-scan line. Then, they travel vertically downward to the upper rough interface and finally reflected back to the sampling point. The initial time of propagation of the wave at each sampling point is the same, and the time information of the echo wave crest carries the distance

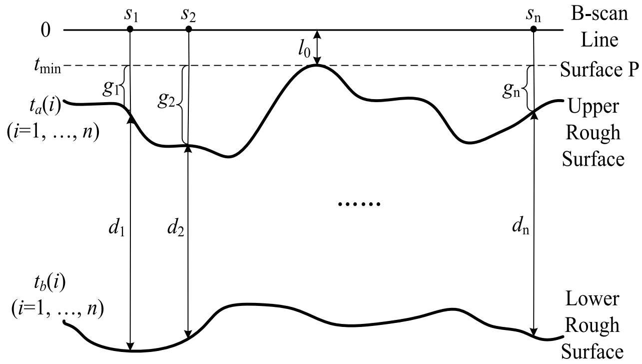

FIGURE 3. Schematic diagram of parameter analysis for the time-delay calibration method.

information between the B-scan line and the upper rough surface. Therefore, the echo shape can reflect the rough surface undulation profile.

The reason why the echo of the lower rough surface cannot reflect the surface profile is that the upper rough surface is not a smooth horizontal surface. For the waves transmitted from the upper rough surface, the heights of sampling points on the upper rough surface are different, and the initial time of transmission from the sampling points on the upper rough surface is different. Therefore, to make the echo of lower surface reflect the surface profile, it is necessary to calibrate the difference in the initial time of propagation in the lower layer of media due to the ups and downs of the upper rough surface. This is the main idea of the time-delay calibration method. The following are the specific steps for implementing this method.

Firstly, the time $t_b(i)$ $(i = 1, \ldots, n)$ at which the echo peak of the lower rough surface is received at each sampling point can be written as

$$t_b(i) = \frac{2l_0}{v_1} + \frac{2g(i)}{v_1} + \frac{2d(i)}{v_2}, \quad i = [1, \ldots, n] \tag{3}$$

where v_1 represents the propagation speed of the wave in medium 1, and v_2 represents the propagation speed of the wave in medium 2.

To calibrate $t_b(i)$ $(i = 1, \ldots, n)$ to make the wave outline reflect the profile of the lower rough surface, it is necessary to eliminate the influence of the roughness of the upper rough surface. Here we artificially modify the rough surface of the upper layer to the smooth horizontal surface P with a distance l_0 from the B-scan line shown in Fig. 3. Thus, $t_b(i)$ $(i = 1, \ldots, n)$ can be calibrated to obtain the time delay $t_c(i)$ $(i = 1, \ldots, n)$ for the calibration method as

$$t_c(i) = t_b(i) - \frac{2g(i)}{v_1} + \frac{2g(i)}{v_2}, \quad i = [1, \ldots, n] \tag{4}$$

where $g(i)$ $(i = 1, \ldots, n)$ are unknown and need to be expressed in known quantities as

$$\frac{2g(i)}{v_1} = t_a(i) - t_{\min}, \quad i = [1, \ldots, n] \tag{5}$$

Furthermore, from equation (2), we can get the following equation

$$\frac{v_1}{v_2} = \frac{\sqrt{\mu_2 \varepsilon_2}}{\sqrt{\mu_1 \varepsilon_1}} \tag{6}$$

Then, we can substitute equation (6) into equation (5) and get

$$\begin{aligned} \frac{2g(i)}{v_2} &= \frac{v_1}{v_2}\left[t_{\mathrm{a}}(i) - t_{\min}\right] \\ &= \frac{\sqrt{\mu_2 \varepsilon_2}}{\sqrt{\mu_1 \varepsilon_1}}\left[t_{\mathrm{a}}(i) - t_{\min}\right], \quad i = [1, \ldots, n] \end{aligned} \tag{7}$$

Then the last revised time delay $t_c(i)$ $(i = 1, \ldots, n)$ can be written as

$$t_c(i) = t_b(i) - \left(1 - \frac{\sqrt{\mu_2 \varepsilon_2}}{\sqrt{\mu_1 \varepsilon_1}}\right)\left[t_{\mathrm{a}}(i) - t_{\min}\right] \quad i = [1, \ldots, n] \tag{8}$$

Equation (8) is the calculation formula of the time-delay calibration method, which can be used to calibrate the echo pattern of the lower rough surface. To ensure the accuracy of the time-delay calibration method, a priori knowledge of the dielectric constant of the layered structure is needed.

C. RESULTS AND DISCUSSION

In this section, we applied the proposed time-delay calibration method to the calibration of the shape of the lower rough surface in the two-layered rough surface structure shown in Fig. 1. The calibrated echo shape will be compared with the profile of the lower rough surface and the echo shape before calibration.

In the simulation of two-layered rough surface scattering, the dimension parameters in the computational model are set to $L_0 = 10$ m, h $= 0.3$ m, $h_0 = 0.15$ m, $d_1 = 0.3$ m, and $d = 0.7$ m. The interval distance spaced between the adjacent sampling points of GPR B-scan is 1 cm, and there are totally 1001 sampling points on the B-scan line. Thus, the obtained B-scan data is composed of 1001 traces of signals. The layers of medium 1 and medium 2 in the model are dry concrete and dry clay. Their relative electrical permittivity ε_{r} and conductivity σ are selected as: 4.0 and 0.005 S/m for dry concrete, and 12.0 and 0.05 S/m for dry clay. The GPR radiating source uses a differential Gaussian pulse with central frequency of 1.5 GHz. To ensure the algorithm's stability and accuracy for FDTD computation [29], the spatial increment is set to $\Delta x = \Delta y = 1$ cm, and the time step is set to $\Delta t = 0.0167$ ns. In order to absorb outward traveling waves, the UPML absorbing boundary with an eight-cell (8 cm) thickness is adopted in the finite difference computation.

Calibration results are presented in Fig. 4. Comparisons are made among the surface's profile, the echo before calibration, and the calibrated echo, as observed in the figure. For the first two figures in Fig. 4, the roughness of the upper surface is different from that of the lower surface. So the

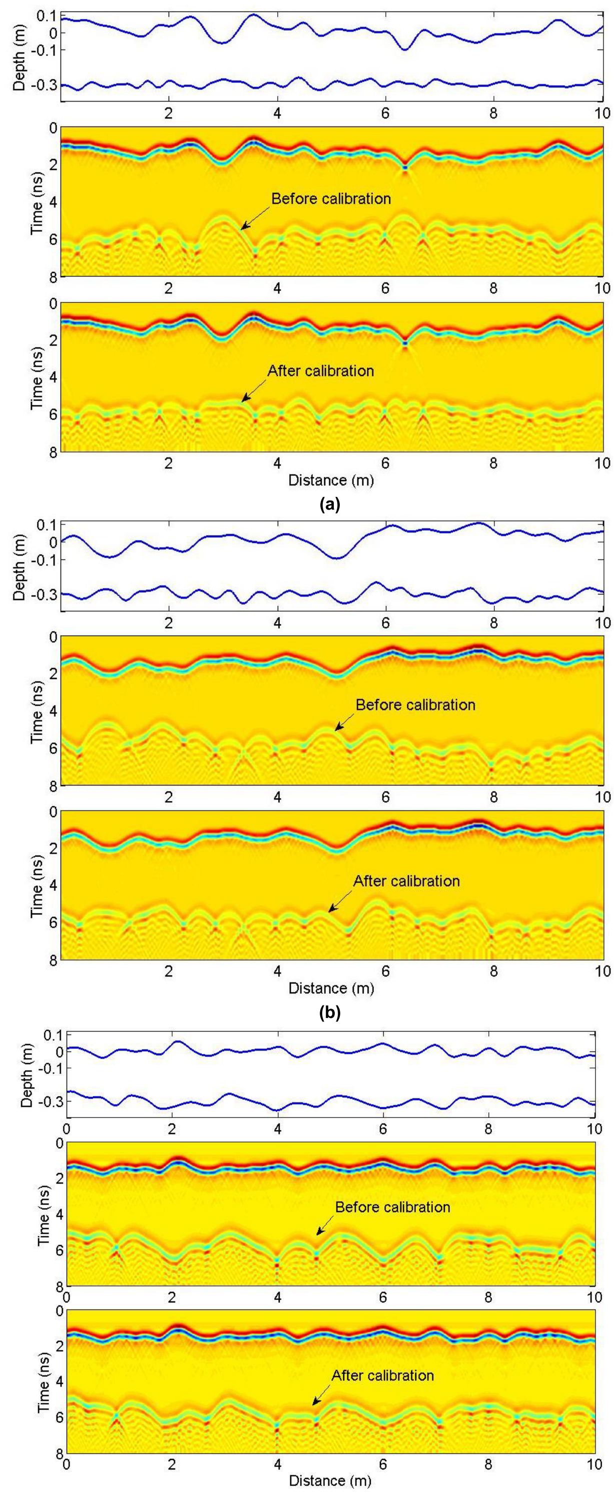

FIGURE 4. Comparisons among the profile of the lower rough surface, the echo before calibration and the echo after calibration with different degrees of roughness: (a) $l = 1.5\lambda$ and $\delta = \lambda$ for the upper layer, $l = \lambda$ and $\delta = 0.4\lambda$ for the lower layer; (b) $l = 2\lambda$ and $\delta = \lambda$ for the upper layer, $l = 1.2\lambda$ and $\delta = 0.6\lambda$ for the lower layer; (c) $l = 1.4\lambda$ and $\delta = 0.6\lambda$ for both of the upper and lower layers; (d) $l = 1.7\lambda$ and $\delta = 0.8\lambda$ for both of the upper and lower layers.

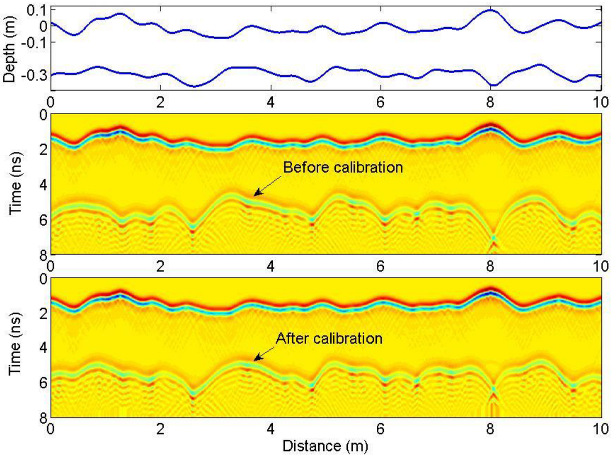

(d)

FIGURE 4. ***(Continued.)*** **Comparisons among the profile of the lower rough surface, the echo before calibration and the echo after calibration with different degrees of roughness: (a) $l = 1.5\lambda$ and $\delta = \lambda$ for the upper layer, $l = \lambda$ and $\delta = 0.4\lambda$ for the lower layer; (b) $l = 2\lambda$ and $\delta = \lambda$ for the upper layer, $l = 1.2\lambda$ and $\delta = 0.6\lambda$ for the lower layer; (c) $l = 1.4\lambda$ and $\delta = 0.6\lambda$ for both of the upper and lower layers; (d) $l = 1.7\lambda$ and $\delta = 0.8\lambda$ for both of the upper and lower layers.**

profile of the upper surface is different from that of the lower surface for the results both in Fig. 4(a) and 4(b). While in Fig. 4(c) and 4(d), the roughness of the upper surface is the same with the roughness of the lower surface. But even so, because the rough surfaces are generated randomly, the profile of the upper rough surface is different from that of the lower rough surface for both the Figs. 4(c) and 4(d). Therefore, the profile of the upper surface is different from the profile of the lower surface in each figure of Fig. 4. Thus, due to the influence of the scattering of the upper surface, the shape of the echo from the lower surface is different from the surface's profile, as observed in each figure of Fig.4. So it is necessary to calibrate the echo shape of the lower rough surface in each case in Fig. 4. From the calibration result of each case in Fig. 4, it can be seen that although the roughness of rough surface varies from case to case, the echo shape of the calibrated lower rough surface is very close to its rough surface profile in all the cases. Moreover, when the upper and lower surfaces have the same roughness (Fig. 4(c) and 4(d)), the difference between the echo shape of the lower rough surface and its profile is not as large as that in the circumstance when the roughnesses of the upper and lower layers are different (Fig. 4(a) and 4(b)). As a result, in the circumstance of the same roughness (Fig. 4(c) and 4(d)), the calibration effect of the echo shape of the lower rough surface is not as significant as that in the circumstance of different roughness (Fig. 4(a) and 4(b)).

In order to further verify the effect of calibration for both the cases of same roughness and different roughnesses of the upper and lower surfaces, we extract the outline curves

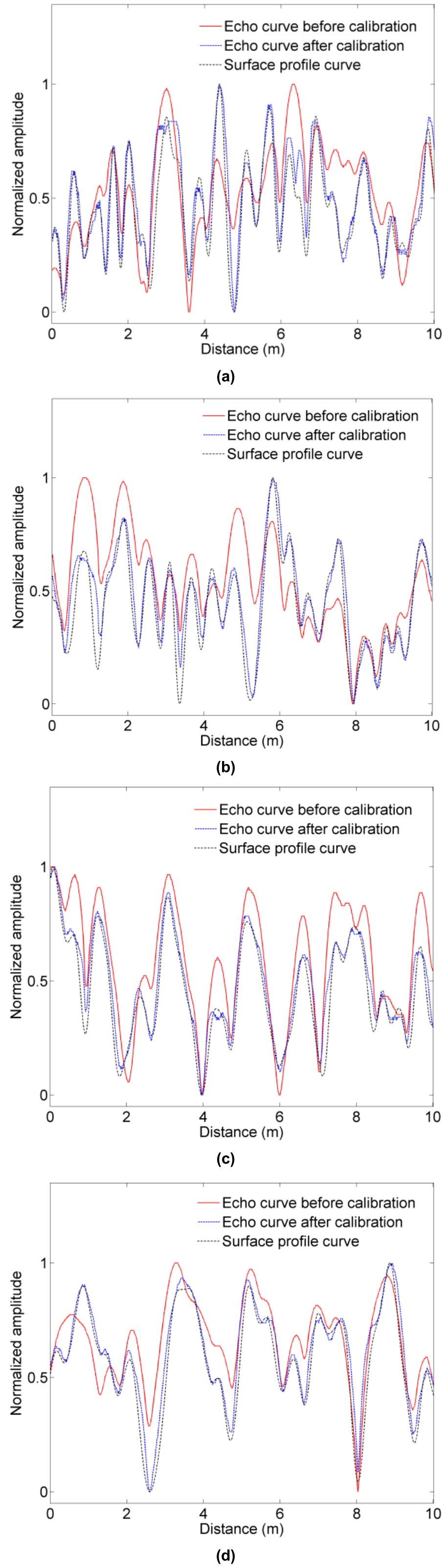

FIGURE 5. **Comparisons among the normalized echo curves before and after calibration and the normalized surface profile curve for the results given in: (a) Fig. 4(a); (b) Fig. 4(b); (c) Fig. 4(c); (d) Fig. 4(d).**

of the echoes from the lower rough surface before and after the calibration respectively. Then the three curves including the extracted echo curves before and after calibration and the profile curve of the lower surface can be collected together to make a comparison. Fig. 5 shows the comparison among the normalized echo curves before and after calibration and the normalized surface profile curve for all the results in Fig. 4. As can be seen from Fig. 5, the echo curve after calibration is much closer to the profile curve than the echo curve before calibration in each figure. The calibrated echo curve shows good agreement with the profile curve for both the circumstances of same roughness and different roughnesses of the upper and lower surfaces. The calibration eliminates the influence of the scattering of the upper surface on the echo shape of the lower surface. The calibrated echo shape can reflect the profile of the lower rough interface in the two-layered rough interface structure.

Using this method, the lower rough surface profile can be observed directly from the radar echo shape. This can help us to obtain the contour fluctuation information of the lower rough surface and subsequently reconstruct the rough surface. Therefore, the time-delay calibration method proposed in this paper is effective for the correction of the echo contour of the lower surface of the two-layered rough surface.

IV. CONCLUSION

A time-delay calibration method for profiling the lower rough interface in the two-layered rough interface structure has been described. Due to the influence of the scattering of the upper rough surface, the echo shape of the lower rough surface is different from the actual profile of the lower rough surface. Using this method, the B-scan echo shape of the lower rough surface can be corrected to reflect the profile of the rough surface. This can help us get the profile shape of the lower rough surface directly and quickly and thus help in the future subsequent estimation and imaging of the profile of the multi-layer rough surface. However, the time-delay calibration method requires a priori knowledge of the dielectric constant of the layered structure to ensure the method's accuracy.

ACKNOWLEDGMENT

Y. Liu thanks Dr. K. Li for his helpful suggestions on program debugging.

REFERENCES

[1] P. Imperatore, A. Iodice, and D. Riccio, "Physical meaning of perturbative solutions for scattering from and through multilayered structures with rough interfaces," *IEEE Trans. Antennas Propag.*, vol. 58, no. 8, pp. 2710–2724, Aug. 2010.

[2] S. Afifi, R. Dusséaux, and A. Berrouk, "Electromagnetic scattering from 3D layered structures with randomly rough interfaces: Analysis with the small perturbation method and the small slope approximation," *IEEE Trans. Antennas Propag.*, vol. 62, no. 10, pp. 5200–5208, Oct. 2014.

[3] A. S. Komarov, J. C. Landy, S. A. Komarov, and D. G. Barber, "Evaluating scattering contributions to c-band radar backscatter from snow-covered first-year sea ice at the winter–spring transition through measurement and modeling," *IEEE Trans. Geosci. Remote Sens.*, vol. 55, no. 10, pp. 5702–5718, Oct. 2017.

[4] H. Zamani, A. Tavakoli, and M. Dehmollaian, "Scattering from two rough surfaces with inhomogeneous dielectric profiles," *IEEE Trans. Antennas Propag.*, vol. 63, no. 12, pp. 5753–5766, Dec. 2015.

[5] H. Zamani, A. Tavakoli, and M. Dehmollaian, "Scattering from layered rough surfaces: Analytical and numerical investigations," *IEEE Trans. Antennas Propag.*, vol. 54, no. 6, pp. 3685–3696, Jun. 2016.

[6] Y. Altuncu, "A numerical method for electromagnetic scattering by 3-D dielectric objects buried under 2-D locally rough surfaces," *IEEE Trans. Antennas Propag.*, vol. 63, no. 8, pp. 3634–3643, Aug. 2015.

[7] A. Martinez-Agirre, J. Álvarez-Mozos, H. Lievens, and N. E. C. Verhoest, "Influence of surface roughness measurement scale on radar backscattering in different agricultural soils," *IEEE Trans. Geosci. Remote Sens.*, vol. 55, no. 10, pp. 5925–5936, Oct. 2017.

[8] S.-Y. He, F.-S. Deng, H.-T. Chen, W.-X. Yu, W.-D. Hu, and G.-Q. Zhu, "Range profile analysis of the 2-D target above a rough surface based on the electromagnetic numerical simulation," *IEEE Trans. Antennas Propag.*, vol. 57, no. 10, pp. 3258–3263, Oct. 2009.

[9] P. Peng, L. X. Guo, and C. Tong, "An EM model for radar multipath simulation and HRRP analysis of low altitude target above electrically large composite scale rough surface," *Electromagnetics*, vol. 38, no. 3, pp. 177–188, 2018.

[10] I. Akduman, R. Kress, and A. Yapar, "Iterative reconstruction of dielectric rough surface profiles at fixed frequency," *Inverse Problems*, vol. 22, no. 3, pp. 939–954, 2006.

[11] A. Yapar, O. Ozdemir, H. Sahinturk, and I. Akduman, "A Newton method for the reconstruction of perfectly conducting slightly rough surface profiles," *IEEE Trans. Antennas Propag.*, vol. 54, no. 1, pp. 275–279, Jan. 2006.

[12] X. Feng, M. Sato, C. Liu, and Y. Zhang, "Profiling the rough surface by migration," *IEEE Geosci. Remote Sens. Lett.*, vol. 6, no. 2, pp. 258–262, Apr. 2009.

[13] T. U. Gurbuz, B. Aslanyurek, E. P. Karabulut, and I. Akduman, "An efficient nonlinear imaging approach for dielectric objects buried under a rough surface," *IEEE Trans. Geosci. Remote Sens.*, vol. 52, no. 5, pp. 3013–3022, May 2014.

[14] S. M. Moghadasi and M. Dehmollaian, "Buried-object time-reversal imaging using UWB near-ground scattered fields," *IEEE Trans. Geosci. Remote Sens.*, vol. 52, no. 11, pp. 7317–7326, Nov. 2014.

[15] S. M. Moghadasi, M. Dehmollaian, and J. Rashed-Mohassel, "Time reversal imaging of deeply buried targets under moderately rough surfaces using approximate transmitted fields," *IEEE Trans. Geosci. Remote Sens.*, vol. 53, no. 7, pp. 3897–3905, Jul. 2015.

[16] D. Comite, F. Ahmad, T. Dogaru, and M. G. Amin, "Adaptive detection of low-signature targets in forward-looking GPR imagery," *IEEE Geosci. Remote Sens. Lett.*, vol. 15, no. 10, pp. 1520–1524, Oct. 2018.

[17] Y. Liu and L.-X. Guo, "B-scan wave outline analysis in numerical modeling of ground-penetrating radar response from layered rough interfaces," *Microw. Opt. Technol. Lett.*, vol. 61, no. 3, pp. 832–837, 2019.

[18] B. Guan, J. F. Zhang, X. Y. Zhou, and T. J. Cui, "Electromagnetic scattering from objects above a rough surface using the method of moments with half-space Green's function," *IEEE Trans. Geosci. Remote Sens.*, vol. 47, no. 10, pp. 3399–3405, Oct. 2009.

[19] A.-Q. Wang, L.-X. Guo, and C. Chai, "Fast numerical method for electromagnetic scattering from an object above a large-scale layered rough surface at large incident angle: Vertical polarization," *Appl. Opt.*, vol. 50, no. 4, pp. 500–508, 2011.

[20] A. Tabatabaeenejad, X. Duan, and M. Moghaddam, "Coherent scattering of electromagnetic waves from two-layer rough surfaces within the Kirchhoff regime," *IEEE Trans. Geosci. Remote Sens.*, vol. 51, no. 7, pp. 3943–3953, Jan. 2013.

[21] N. Dechamps and C. Bourlier, "Electromagnetic scattering from a rough layer: Propagation-inside-layer expansion method combined to an updated BMIA/CAG approach," *IEEE Trans. Antennas Propag.*, vol. 55, no. 10, pp. 2790–2802, Oct. 2007.

[22] C. Bourlier, C. L. Bastard, and V. Baltazart, "Generalization of PILE method to the EM scattering from stratified subsurface with rough interlayers: Application to the detection of debondings within pavement structure," *IEEE Trans. Geosci. Remote Sens.*, vol. 53, no. 7, pp. 4104–4115, Jul. 2015.

[23] C. Jia, L. Guo, and P. Yang, "EM scattering from a target above a 1-D randomly rough sea surface using GPU-based parallel FDTD," *IEEE Antennas Wireless Propag. Lett.*, vol. 14, pp. 217–220, 2015.

[24] I. Giannakis, A. Giannopoulos, and C. Warren, "A realistic FDTD numerical modeling framework of ground penetrating radar for landmine detection," *IEEE J. Sel. Topics Appl. Earth Observ. Remote Sens.*, vol. 9, no. 1, pp. 37–51, Jan. 2016.
[25] C. Wu, X. Zhang, and G. Fang, "Bistatic scattering from three-dimensional layered structures with multilayer rough interfaces," *IEEE Geosci. Remote Sens. Lett.*, vol. 11, no. 3, pp. 676–680, Mar. 2014.
[26] H. Zamani, A. Tavakoli, and M. Dehmollaian, "Scattering by a dielectric sphere buried in a half-space with a slightly rough interface," *IEEE Trans. Antennas Propag.*, vol. 66, no. 1, pp. 347–359, Jan. 2018.
[27] M. Sanamzadeh, L. Tsang, and J. T. Johnson, "3-D electromagnetic scattering from multilayer dielectric media with 2-D random rough interfaces using T-matrix approach," *IEEE Trans. Antennas Propag.*, vol. 67, no. 1, pp. 495–503, Jan. 2019.
[28] Y. Kuga and P. Phu, "Experimental studies of millimeter-wave scattering in discrete randommedia and from rough surfaces," *Prog. Electromagn. Res.*, vol. 14, pp. 37–88, 1996.
[29] J. S. Juntunen and T. D. Tsiboukis, "Reduction of numerical dispersion in FDTD method through artificial anisotropy," *IEEE Trans. Microw. Theory Techn.*, vol. 48, no. 4, pp. 582–588, Apr. 2000.

YING LIU (S'16) received the M.S. degree in underwater acoustic engineering from Harbin Engineering University, in 2006. She is pursuing the Ph.D. degree with Xidian University. She is currently an Assistant Professor with the Tianjin University of Technology and Education, Tianjin, China. Her current research interests include electromagnetic wave scattering modeling, microwave imaging, and computational electromagnetics.

LIXIN GUO (S'95–M'03–SM'16) received the M.S. degree in radio science from Xidian University, Xi'an, China, and the Ph.D. degree in astrometry and celestial mechanics from the Chinese Academy of Sciences, China, in 1993 and 1999, respectively.

From 2001 to 2002, he was a Visiting Scholar with the School of Electrical Engineering and Computer Science, Kyungpook National University, Daegu, South Korea. He has also been a Visiting Professor with d'Energetique des Systemes et Precedes (LESP), University of Rouen, Mont-Saint-Aignan, France, and Faculty of Engineering and Physical Sciences, University of Manchester, Manchester, U.K. He has been a Chief Professor of Innovative Research Team in Shaanxi Province, China, since 2014. He is currently a Professor and the Head of the School of Physics and Optoelectronic Engineering, Xidian University, China. He has been in charge of and undertaken more than 30 projects. He has authored and coauthored four books and over 300 journal papers. His research interests include electromagnetic wave propagation and scattering in complex and random media, computational electromagnetics, inverse scattering, and antenna analysis and design.

Prof. Guo is a fellow of the Chinese institute of Electronics (CIE) and a fellow of the Physics Institute of Shaanxi Province, China. He was a recipient of the National Science Fund for Distinguished Young Scholars, in 2012, and a Distinguished Professor of Changjiang Scholars Program, in 2014.